

1
2
3
4
5
6
7
8
9
10
11
12
13
14
15
16
17
18
19
20
21
22

REVISION 2

Strontiohurlbutite, SrBe₂(PO₄)₂, a new mineral from Nanping No. 31 pegmatite, Fujian Province, Southeastern China

CAN RAO^{1,2,*}, RUCHENG WANG¹, FRÉDÉRIC HATERT³, XIANGPING GU⁴, LUISA OTTOLINI⁵,
HUAN HU¹, CHUANWAN DONG², FABRICE DAL BO³, AND MAXIME BAIJOT³

¹ State Key Laboratory for Mineral Deposits Research, School of Earth Sciences and
Engineering, Nanjing University, Nanjing 210093, P.R. China

² Department of Earth Sciences, Zhejiang University, Hangzhou 310027, P.R. China

³ Laboratoire de Minéralogie, B18, Université de Liège, B-4000 Liège, Belgium

⁴ School of Earth Sciences and Info-physics, Central South University, Changsha, Hunan
410083, P.R. China

⁵ C.N.R.–Istituto di Geoscienze e Georisorse (IGG), Unità di Pavia, Via A. Ferrata 1, I-27100
Pavia, Italy

* E-mail: canrao@zju.edu.cn

23

ABSTRACT

24 Strontiohurlbutite, ideally $\text{SrBe}_2(\text{PO}_4)_2$, is a new member of hurlbutite group discovered
25 in the Nanping No. 31 pegmatite, Fujian province, southeastern China. Crystals are mainly
26 found in zones I, II and IV; they are platy, subhedral to anhedral, with a length from 5 μm to
27 1.5 mm. Associated minerals mainly include quartz, muscovite, beryl, hurlbutite,
28 hydroxylherderite, apatite-group minerals, and phenakite. Strontiohurlbutite crystals are light
29 blue, translucent to transparent, and have vitreous luster. The Mohs hardness is about 6, and
30 the tenacity is brittle. Optically, strontiohurlbutite is biaxial (-), $\alpha = 1.563(3)$, $\beta = 1.569(2)$, γ
31 $= 1.572(3)$ (white light), $2V_{\text{meas}} = 68.5(5)^\circ$, and exhibits weak dispersion, $r > v$. The optical
32 orientation is $X = \mathbf{b}$, $Y \approx \mathbf{c}$. Electron-microprobe and SIMS analyses (average of 16) give SrO
33 29.30, P_2O_5 51.05, CaO 0.91, BaO 0.64, and BeO 17.71 wt%; total 99.61 wt%. The empirical
34 formula, based on 8 O apfu, is $(\text{Sr}_{0.81}\text{Ca}_{0.05}\text{Ba}_{0.01})_{\Sigma 0.87}\text{Be}_{2.02}\text{P}_{2.05}\text{O}_8$. The stronger eight lines of
35 the measured X-ray powder-diffraction pattern [d in $\text{\AA}(l)(hkl)$] are: 3.554(100)(121);
36 3.355(51)(211); 3.073(38)(022); 2.542(67)(113); 2.230(42) (213); 2.215(87)(32 $\bar{1}$);
37 2.046(54)(223); 1.714(32)(143). Strontiohurlbutite is monoclinic, space group $P2_1/c$; unit-cell
38 parameters refined from single-crystal X-ray diffraction data are: $a = 7.997(3)$, $b = 8.979(2)$, c
39 $= 8.420(7)$ \AA , $\beta = 90.18(6)^\circ$, $V = 604.7(1)$ \AA^3 ($Z = 4$, calculated density = 3.101 g/cm^3). The
40 mineral is isostructural with hurlbutite, $\text{CaBe}_2(\text{PO}_4)_2$, and with paracelsian, $\text{BaAl}_2\text{Si}_2\text{O}_8$. The
41 formation of strontiohurlbutite is related to the hydrothermal alteration of primary beryl by
42 late Sr- and P-rich fluids.

43 **Keywords:** Strontiohurlbutite, $\text{SrBe}_2(\text{PO}_4)_2$, new mineral, hurlbutite, Nanping No. 31
44 pegmatite, Fujian province, China

45

46

47

INTRODUCTION

48 The new mineral strontiohurlbutite, a Sr-dominant analog of hurlbutite, was discovered in
49 the Nanping No. 31 pegmatite, Fujian province, southeastern China. Polarizing microscopy,
50 electron-microprobe analyses, X-ray diffraction measurements, Raman spectroscopy, and
51 Secondary-ion Mass Spectrometry (SIMS), were used to determine its petrographic features,
52 chemical composition and crystal structure. The species and the name have been approved by
53 the International Mineralogical Association, Commission on New Minerals, Nomenclature
54 and Classification (CNMNC) (IMA 2012-032) (Williams et al. 2012). The co-type specimen
55 used for the electron-microprobe analyses, X-ray powder diffraction, XPS, Raman and
56 optical measurements is deposited at the Geological Museum of China, Beijing, China,
57 catalogue number M11803. The co-type sample used for the single-crystal structure
58 measurements is stored at the Laboratory of Mineralogy, University of Liège, catalogue
59 number 20387. This paper presents the occurrence of this new Sr phosphate with the
60 hurlbutite-type structure, and discusses the origin of strontiohurlbutite in the Nanping
61 pegmatite.

62

63

OCCURRENCE AND PARAGENESIS

64 Strontiohurlbutite was found in the Nanping No. 31 pegmatite, Fujian Province,
65 southeastern China, which is located at longitude E 118°06', latitude N 26°40', about 8 km
66 west of the Nanping city. The No. 31 pegmatite is a highly evolved and well-zoned pegmatite

67 in the Nanping pegmatite district. Five discontinuous mineralogical-textural zones were
68 distinguished from the outermost zone inward (Yang et al. 1987): quartz – albite – muscovite
69 zone (Zone I), saccharoidal albite ± muscovite zone (Zone II); quartz – coarse albite –
70 spodumene zone (Zone III); quartz – spodumene – amblygonite zone (Zone IV); and blocky
71 quartz – K-feldspar zone (Zone V). The petrography and mineral paragenesis of different
72 textural zones in this pegmatite have been well described in previous publications (e.g., Yang
73 et al. 1987; Rao et al. 2009, 2011). Strontiohurlbutite was found in samples from zones I, II
74 and IV.

75 Strontiohurlbutite from zone I forms subhedral to euhedral crystals up to to 1.5 mm long,
76 mainly in close association with quartz (Fig. 1a). Back-scattered electron (BSE) images show
77 the crystals to be weakly heterogeneous (Fig. 1a), and the brighter areas are slightly richer in
78 Sr than the darker areas. Other associated minerals include muscovite, fluorapatite, and
79 hurlbutite. In zone II, strontiohurlbutite occurs as small aggregates about 5 to 100 µm across.
80 They are closely associated with beryl, hurlbutite, hydroxylherderite, fluorapatite, and
81 phenakite, forming the Be silicate + phosphate mineral associations interstitial to albite
82 crystals (Fig. 1b, Rao et al. 2011: Fig. 4a, the brightest areas). In zones I and IV,
83 strontiohurlbutite also forms aggregates with a size ranging from 2 to 50 µm; it surrounds
84 hurlbutite crystals from zone I, and is distributed along the fractures of Cs-rich beryl from
85 zone IV (Fig. 1c). Other secondary phases observed in this aggregates include beryl,
86 hurlbutite, hydroxylapatite and muscovite.

87

88

PHYSICAL AND OPTICAL PROPERTIES

89 Strontiohurlbutite forms platy, subhedral crystals and anhedral grains. More than 50
90 grains were found in zones I and II; they are light blue, transparent to translucent, and have
91 vitreous luster. The Mohs hardness is about 6, the tenacity is brittle, and no cleavage was
92 observed. The calculated density, based on the empirical formula and single-crystal unit cell
93 parameters, is 3.101 g/cm³. Optically, strontiohurlbutite is biaxial negative, with $\alpha = 1.563$ (2),
94 $\beta = 1.569$ (2), $\gamma = 1.572$ (3), measured in white light. The $2V$ angle, measured directly by
95 conoscopic observations, is 68.5 (5)°; the calculated $2V$ is 70°. It exhibits weak dispersion,
96 $r > v$, and it is colorless. The optical orientation is $X = \mathbf{b}$, $Y \approx \mathbf{c}$, and pleochroism is absent.
97 Based on the calculated density and the measured indices of refraction, the compatibility
98 index $[1 - (K_p/K_c)]$ is -0.006, and corresponds to the “Superior” category (Mandarino 1981).

99

100

RAMAN SPECTROSCOPY

101

102

103

104

105

106

107

108

109

110

Raman spectra of strontiohurlbutite were collected using a Renishaw RM2000 Laser Raman microprobe in the State Key Laboratory for Mineral Deposits Research at Nanjing University. A 514.5 nm Ar⁺ laser with a surface power of 5 mW was used for exciting the radiation. Silicon (520 cm⁻¹ Raman shift) was used as a standard. Raman spectra were acquired from 100 to 1000 cm⁻¹ and the accumulation time of each spectrum is 60 s. Raman spectra were collected on single crystals of strontiohurlbutite on polished thin section chips. Figure 2 shows the Raman spectrum of strontiohurlbutite, which is remarkably similar to the spectrum of hurlbutite (<http://rruff.info/hurlbutite/display=default/R070612>), confirming the structural similarity between strontiohurlbutite and hurlbutite. The Raman spectrum contains strong sharp peaks at 1022 cm⁻¹, medium sharp peaks at 587, 575, 550, 442, 343 and 204 cm⁻¹,

111 and weak sharp peaks at 1178, 1135, 492, 421 and 176 cm^{-1} , respectively. The Raman shifts
112 of (PO_4) groups were observed at 1022 (ν_1), 421, 442(ν_2), 1135, 1178 (ν_3) and 550, 575 and
113 587 cm^{-1} (ν_4). The Be-O vibration modes are probably at 204 and 492 cm^{-1} , and the Raman
114 shifts at 176 and 343 cm^{-1} certainly correspond to Sr-O vibrations.

115

116

CHEMICAL COMPOSITION

117 The chemical composition of strontiohurlbutite (Table 1) was obtained with a JEOL
118 JXA-8100M electron microprobe (WDS mode, 15 kV, 20 nA, beam diameter 1 μm) at the
119 State Key Laboratory for Mineral Deposits Research, Nanjing University. The following
120 standards were used: synthetic $\text{Ba}_3(\text{PO}_4)_2$ (Ba $L\alpha$, P $K\alpha$), synthetic SrSO_4 (Sr $L\alpha$), and
121 hornblende (Ca $K\alpha$).

122 To determine the BeO content of strontiohurlbutite, SIMS measurements were
123 performed with a Cameca IMS-4F ion microprobe installed at CNR-IGG, Pavia (Italy). The
124 experimental conditions are similar to those reported in the literature (Ottolini et al. 1993,
125 2002; Hatert et al. 2011). We selected a sample of beryllonite (*courtesy* of S. Filippo,
126 Natural History Museum of Luxembourg) as standard for Be. The calibration factor for Be in
127 the standard was obtained through the calculation of the experimental Be ion yield, having
128 chosen P as the inner element for the matrix. We thus derived the IY(Be/P), defined as
129 $(\text{Be}^+/\text{P}^+)/((\text{Be}(\text{at})/\text{P}(\text{at})))$ where Be^+ and P^+ are the current intensities detected at the electron
130 multiplier and (at) is the elemental atomic concentration. The IY (Be/P) was then used to
131 calculate the Be concentration in the strontiohurlbutite, resulting in $17.71 \pm 0.464(1\sigma)$ BeO

132 wt%. Additionally, a few H₂O about 0.066±0.010(1σ) wt% is detected in strontiohurlbutite;
133 lithium is absent.

134 Representative analyses of strontiohurlbutite (Table 1) lead to the empirical formula
135 (Sr_{0.81}Ca_{0.05}Ba_{0.01})_{Σ0.87}Be_{2.02}P_{2.05}O₈, based on 8 O atoms per formula unit. The idealized,
136 end-member formula is SrBe₂(PO₄)₂, which requires 35.06 wt% SrO, 16.92 wt% BeO, and
137 48.02 wt% P₂O₅; total 100.00 wt. %. A careful examination of chemical data (Table 1)
138 indicates significant amounts of Ca and Ba, reaching 3.10 wt% CaO and 0.22 wt% BaO, in
139 strontiohurlbutite from zone IV. This indicates the existence of a possible solid solution
140 between hurlbutite and strontiohurlbutite; such a solid solution is confirmed by the high Sr
141 contents observed in some hurlbutite grains, reaching 10 wt% SrO.

142

143

144

X-RAY POWDER DIFFRACTION

145 The X-ray powder diffraction pattern of strontiohurlbutite was collected using
146 micro-diffraction data on 5 crystals, with a RIGAKU D/max Rapid IIR micro-diffractometer
147 (CuKα, λ = 1.54056 Å) at the School of Earth Sciences and Info-physics, Central South
148 University, China. The micro-diffractometer was operated under these conditions: 48 kV, 250
149 mA, 0.05 mm collimator diameter, and 5-hours exposure time. The hurlbutite-based
150 structural model (Huminicki and Hawthorne 2002), in which Ca sites are occupied by Sr
151 atoms, was used to index the powder diffraction data. Table 2 shows the main indexed
152 micro-diffraction data of strontiohurlbutite. The stronger eight lines of the measured X-ray
153 powder-diffraction pattern [*d* in Å(*I*)(*hkl*)] are: 3.554(100)(121); 3.355(51)(211);

154 3.073(38)(022); 2.542(67)(113); 2.230(42) (213); 2.215(87)(32 $\bar{1}$); 2.046(54)(223);
155 1.714(32)(143). The X-ray powder diffraction studies on the crystals of strontiohurlbutite
156 gave the following unit-cell parameters: $a = 8.005$ (4), $b = 8.998$ (5), $c = 8.426$ (5) Å, $\beta =$
157 90.05 (5)°, $V = 606.9$ (3) Å³, $Z = 4$, and space group $P 2_1/c$.

158

159 CRYSTAL STRUCTURE DETERMINATION

160

161 The X-ray intensity data, aimed to perform a structure refinement of strontiohurlbutite,
162 were collected on an Agilent Technologies Xcalibur four-circle diffractometer, equipped with
163 an EOS CCD area-detector (University of Liège, Belgium) on a crystal fragment measuring
164 $0.35 \times 0.35 \times 0.18$ mm. A total of 2186 frames with a spatial resolution of 1° were collected
165 by the φ/ω scan technique, with a counting time of 10 s per frame, in the range $6.64^\circ < 2\theta <$
166 58.18° . A total of 26214 reflections were extracted from these frames, corresponding to 1566
167 unique reflections. Unit-cell parameters refined from these reflections are a 7.997(1), b
168 8.979(1), c 8.420(1) Å, β 90.18(1)°, V 604.7(1)Å³, space group $P2_1/c$, in good agreement with
169 those refined from the powder-diffraction data. A summary of the crystal data is presented in
170 Table 3. The data were corrected for Lorentz, polarization and absorption effects, the latter
171 with an empirical method using the SCALE3 ABSPACK scaling algorithm included in the
172 CrysAlisRED package (Oxford Diffraction 2007). The structure refinement was performed with
173 anisotropic-displacement parameters for all atoms. The final conventional R_1 factor [$F_0 >$
174 $2\sigma(F_0)$] is 0.0197. Atomic coordinates and anisotropic displacement parameters, as well as
175 selected bond distances and angles, are given in Table 4 and Table 5, respectively.

176 The structure of strontiohurlbutite is based on a tetrahedral framework consisting of
177 corner-sharing BeO_4 and PO_4 tetrahedra (Fig. 3). BeO_4 and PO_4 tetrahedra are assembled in
178 4- and 8-membered rings, respectively. The 4-membered ring consists of a pair of tetrahedra
179 pointing upwards (U) and a pair of tetrahedra pointing downwards (D), showing the UUDD
180 type rings (Fig. 4a); the 8-membered ring shows the DDUDUUDU pattern (Fig. 4b). Sr
181 atoms are localized in the channels formed by the alignment of the 8-membered rings (Fig. 3).
182 A view perpendicular to the b direction shows that BeO_4 and PO_4 tetrahedra connected by
183 corner-sharing form a double crankshaft chain running along a (Fig. 4c).

184 The Sr^{2+} ions are located in 10-coordinated polyhedra, characterized by 7 short bonds
185 [$\langle \text{Sr-O} \rangle = 2.596(2) \text{ \AA}$] and 3 long bonds [$\langle \text{Sr-O} \rangle = 3.227(2) \text{ \AA}$]. This polyhedron can be
186 described as a combination of a square pyramid and of a trigonal prism, with one square face
187 in common. Based on the empirical parameters of Brown and Altermatt (1965), the
188 bond-valence sums for strontiohurlbutite were calculated (Table 6). The bond-valence sums
189 for P (5.00-5.04), Be (2.05-2.07), and Sr (2.09) are very close to the theoretical values.

190 The structure of strontiohurlbutite can be compared to those of hurlbutite (Mrose 1952;
191 Bakakin and Belov 1959; Lindbloom et al. 1974) and paracelsian (Smith 1953; Bakakin and
192 Belov 1960). The replacement of Ca in the structure of hurlbutite (effective ionic radius 1.06
193 \AA ; Shannon 1976) by Sr in strontiohurlbutite (effective ionic radius 1.21 \AA) leads to an
194 increase of the seven shorter M^{2+} -O bonds from 2.469(6) \AA to 2.596(2) \AA , respectively. This
195 larger crystallographic site also implies an increase of the unit-cell parameters of
196 strontiohurlbutite, compared to those of hurlbutite (Table 7).

197

198

ORIGIN AND SIGNIFICANCE

199 Strontium is a widespread element in most rocks. Since its crystal-chemistry is similar to
200 that of calcium, Sr commonly substitutes for Ca in minerals, especially in phosphates.
201 Various Sr-bearing phosphate minerals, including stronadelphite (Pekov et al. 2010),
202 palermoite (Mrose 1953; Ni et al. 1993), goedkenite (Moore et al. 1975), and
203 strontiohurlbutite (Britvin et al. 1991), are known to have a Ca-bearing isostructural
204 analogue. The new mineral species described in the present paper, strontiohurlbutite, is the
205 Sr-dominant analogue of hurlbutite, and constitutes a new member of the hurlbutite group
206 (Table 7).

207 Strontiohurlbutite occurs in close association with hurlbutite, thus indicating that both
208 minerals may crystallize under a comparable range of physicochemical conditions. Their
209 textural relationships suggest that the hurlbutite-group minerals evolved from hurlbutite to
210 strontiohurlbutite. Strontiohurlbutite crystals are enriched in Ba in zones I-II and in Ca in
211 zone IV (Table 1), thus indicating a solid solution with hurlbutite. Consequently, the activity
212 of Sr in the pegmatite fluids seems to be an essential factor controlling the crystallization of
213 strontiohurlbutite.

214 High Sr activity in late hydrothermal fluids affecting pegmatite systems was documented
215 in the literature (e.g., Moore 1982; Charoy et al. 2003). This high activity induces the
216 replacement of early minerals by secondary Sr-bearing minerals such as palermoite and
217 goyazite (e.g., Ni et al. 1993; Galliski et al. 2012). In the Nanping No. 31 pegmatite,
218 strontiohurlbutite occurs with hurlbutite along fractures of primary beryl (Fig. 1c); this
219 petrographic texture indicates that the primary beryl was affected by a late Sr-, Ca- and P-rich

220 hydrothermal fluid. Hurlbutite contains high SrO contents, from 5 to 10 wt%, thus indicating
221 that Sr in the late hydrothermal fluids became a trigger for the transition from hurlbutite to
222 strontiohurlbutite. In fact, other secondary Sr-bearing phosphate minerals such as palermoite,
223 goyazite, hydroxylapatite, and bertossaite were found in the Nanping No. 31 pegmatite (Ni et
224 al. 1993; Yang et a. 1994); the source of Sr in the hydrothermal fluids, responsible for the
225 crystallization of these secondary minerals, remains to be determined in the future.

226

227

228

ACKNOWLEDGMENTS

229 Financial support for the research was provided by NSF of China (Grant No. 41102020,
230 41230315), the Ministry of Science and Technology (Grant No. 2012CB416704), and by the
231 Fundamental Research Funds for the Central Universities. We are indebted to CHEN Guojian
232 (Geological Survey of North Fujian) for his help during field work.

233

234

235

REFERENCES CITED

236 Bakakin, V.V. and Belov, N.V. (1959) The crystalline structure of hurlbutite. Doklady Akademii Nauk
237 SSSR, 125, 343-344.

238 Bakakin, V.V. and Belov, N.V. (1960) Crystal structure of paracelsian, Soviet Physics Crystallography,
239 5, 826-829.

- 240 Britvin, S.N., Pakhomovskii, Y.A., Bogdanova, A.N. and Skiba, V.I. (1991) Strontio whitlockite,
241 $\text{Sr}_9\text{Mg}(\text{PO}_3\text{OH})(\text{PO}_4)_6$, a new mineral species from the Kovdor Deposit, Kola Peninsula, U.S.S.R.
242 Canadian Mineralogist, 29, 87-93.
- 243 Brown, I.D. and Altermatt, D. (1965) Bond-valence parameters obtained from a systematic analysis of
244 the inorganic crystal structure database. Acta Crystallographica, B41, 244-247.
- 245 Charoy, B., Chaussidon, M., Carlier De Veslud, C.L. and Duthou, J.L. (2003) Evidence of Sr mobility
246 in and around the albite-lepidolite-topaz granite of Beauvoir (France): an in-situ ion and electron
247 probe study of secondary Sr-rich phosphates. Contributions to Mineralogy and Petrology, 145,
248 673-690.
- 249 Galliski, M.Á., Černý, P., Márquez-Zavalía, M.F. and Chapman, R. (2012) An association of
250 secondary Al-Li-Be-Ca-Sr phosphates in the San Elías pegmatite, San Luis, Argentina. Canadian
251 Mineralogist, 50, 933-942.
- 252 Hatert, F., Ottolini, L. and Schmid-Beurmann, P. (2011) Experimental investigation of the alluaudite
253 + triphylite assemblage, and development of the Na-in-triphylite geothermometer: applications to
254 natural pegmatite phosphates. Contributions to Mineralogy and Petrology, 161, 531-546.
- 255 Huminicki, D.M.C. and Hawthorne, F.C. (2002) The Crystal Chemistry of the Phosphate Minerals.
256 Reviews in Mineralogy and Geochemistry, 48, 123-253.
- 257 Lindbloom, J.T., Gibbs, G.V. and Ribbe, P.H. (1974) The crystal structure of hurlbutite: a comparison
258 with danburite and anorthite. American Mineralogist, 59, 1267-1271.
- 259 Mandarino, J.A. (1981) The Gladstone-Dale relationship. IV. The compatibility concept and its
260 application. Canadian Mineralogist, **19**, 441-450.

- 261 Moore, P.B. (1982) Pegmatite minerals of P(V) and B(III). in Granitic Pegmatites in Science and
262 Industry (P. Černý, ed.). Mineralogical Association of Canada Short Course Handbook E,
263 267-291.
- 264 Moore, P.B., Irving, A.J. and Kampf, A.R. (1975) Foggite, $\text{CaAl}(\text{OH})_2(\text{H}_2\text{O})[\text{PO}_4]$; goedkenite,
265 $(\text{Sr,Ca})_2\text{Al}(\text{OH})[\text{PO}_4]_2$; and samuelsonite, $(\text{Ca,Ba})\text{Fe}^{2+}_2\text{Mn}^{2+}_2\text{Ca}_8\text{Al}_2(\text{OH})_2[\text{PO}_4]_{10}$: three new
266 species from the Palermo No. 1 pegmatite, North Groton, New Hampshire. American
267 Mineralogist, 60, 957-964.
- 268 Mrose, M.E. (1952) Hurlbutite, $\text{CaBe}_2(\text{PO}_4)_2$, a new mineral. American Mineralogist, 37, 931-940.
- 269 Mrose, M.E. (1953) Palermoite and goyazite, two strontium minerals from the Palermo mine, North
270 Groton, N H. (abstr.). American Mineralogist, 38, 354.
- 271 Ni, Y.X., Yang, Y.Q. and Wang, W.Y. (1993) Palermoite-bertossaite in Nanping granitic pegmatites,
272 Fujian. Acta mineralogica sinica, 13(4), 346-353 (in Chinese with English abstract).
- 273 Ottolini, L., Bottazzi, P. and Vannucci, R. (1993): Quantification of Lithium, Beryllium and Boron in
274 Silicates by Secondary Ion Mass Spectrometry Using Conventional Energy Filtering, Analytical
275 Chemistry, 65, 1960-1968.
- 276 Ottolini, L., Camara, F., Hawthorne, F.C. and Stirling, J. (2002): SIMS matrix effects in the analysis
277 of light elements in silicate minerals: Comparison with SREF and EMPA data, American
278 Mineralogist, 87, (2002), 1477-1485.
- 279 Oxford Diffraction (2007) *CrysAlis CCD and CrysAlis RED, version 1.71*. Oxford Diffraction, Oxford,
280 England.
- 281 Pekov, I.V., Britvin, S.N., Zubkova, N.V., Pushcharovsky, D.Y., Pasero, M. and Merlino, S. (2010)
282 Stronadelphite, $\text{Sr}_5(\text{PO}_4)_3\text{F}$, a new apatite-group mineral. European journal of Mineralogy, 22(6),
283 869-874.

- 284 Rao, C., Wang, R.C. and Hu, H. (2011) Paragenetic assemblages of beryllium silicates and
285 phosphates from the Nanping no. 31 granitic pegmatite dyke, Fujian province, southeastern
286 china. *Canadian Mineralogist*, 49(5), 1175-1187.
- 287 Rao, C., Wang, R.C., Hu, H. and Zhang, W.L. (2009) Complex internal textures in oxide minerals
288 from the Nanping No. 31 dyke of granitic pegmatite, Fujian province, Southeastern China.
289 *Canadian Mineralogist*, 47, 1195-1212.
- 290 Shannon, R.D. (1976) Revised effective ionic radii and systematic studies of interatomic distances in
291 halides and chalcogenides. *Acta Crystallographica*, A32, 751-767.
- 292 Smith, J.V. (1953) The crystal structure of paracelsian, $BaAl_2Si_2O_8$. *Acta Crystallographica*, 6,
293 613-620.
- 294 Williams, P. A., Hatert, F., Pasero, M. and Mills, S. J. (2012): New minerals and nomenclature
295 modifications approved in 2012, *Mineralogical Magazine*, 76, 1281-128.
- 296 Yang, Y.Q., Ni, Y.X., Guo, Y.Q., Qiu, N.M., Chen, C.H., Cai, C.F., Zhang, Y.P., Liu, J.B. and Chen,
297 Y.X. (1987) Rock-forming and ore-forming characteristics of the Xikeng granitic pegmatites in
298 Fujian Province. *Mineral Deposits*, 6(3), 10-21 (in Chinese with English abstract).
- 299 Yang, Y.Q., Wang, W.Y., Lin G.X., Chen, C.H. and Zhu, J.H. (1994) Phosphate minerals and their
300 geochemical evolution of granitic pegmatite in Nanping, Fujian Province. *Geology of Fujian*,
301 13(4), 215-226 (in Chinese with English abstract).

302

303

304

305

306

307

FIGURE CAPTIONS

308

309 **FIGURE 1.** BSE images showing occurrence and mineral associations of strontiohurlbutite. (a)
310 euhedral strontiohurlbutite crystals in close association with quartz in zone I. (b) Small
311 aggregate of strontiohurlbutite in a Be silicate + phosphate assemblage interstitial to albite
312 crystals in zone II. (c) Strontiohurlbutite associated with secondary phases (beryl, hurlbutite,
313 hydroxylapatite and muscovite) in the fractures of primary beryl from zone IV. Abbr.: Qz -
314 quartz, Srh - strontiohurlbutite, Brl-P - primary beryl, Brl-S - secondary beryl, Phn -
315 phenakite, Ab - albite, Hlb - hurlbutite, Ms - muscovite, Ap - apatite.

316

317 **FIGURE 2.** The Raman spectrum of strontiohurlbutite.

318

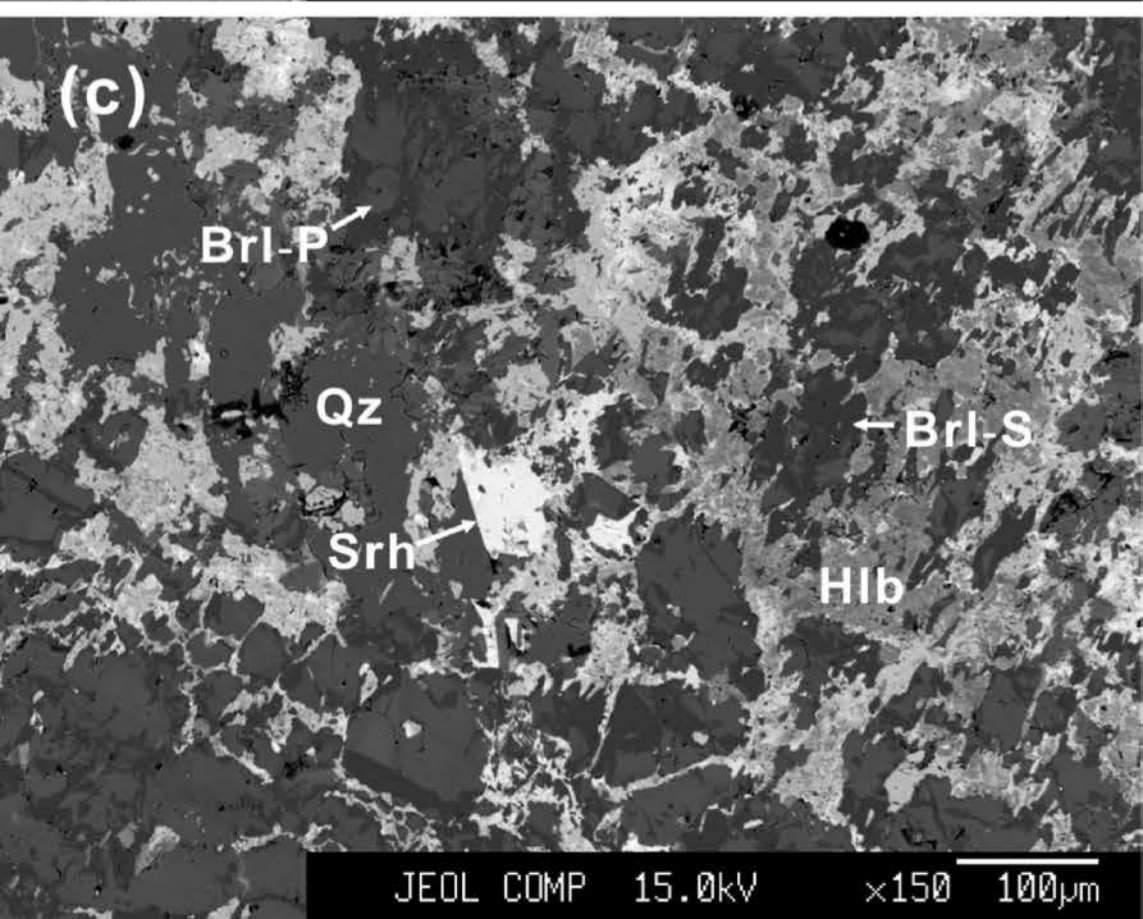
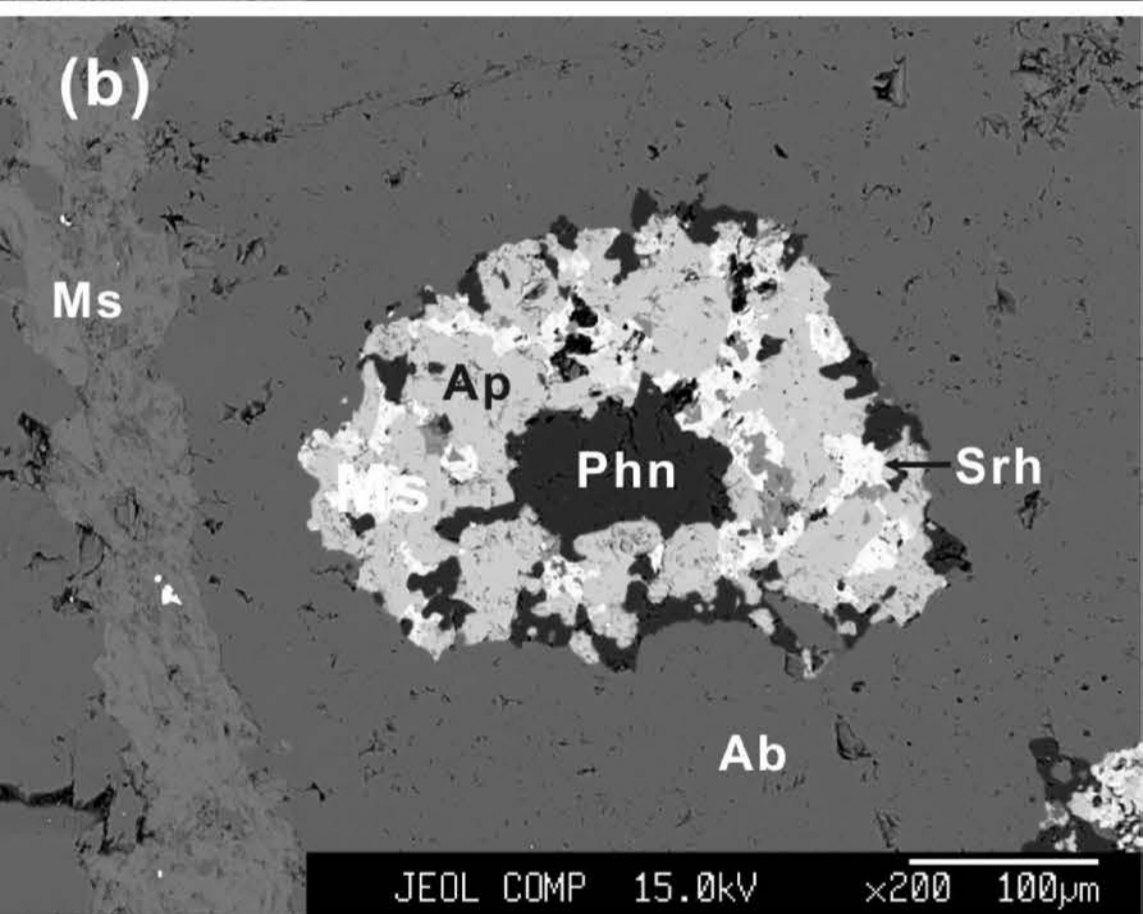
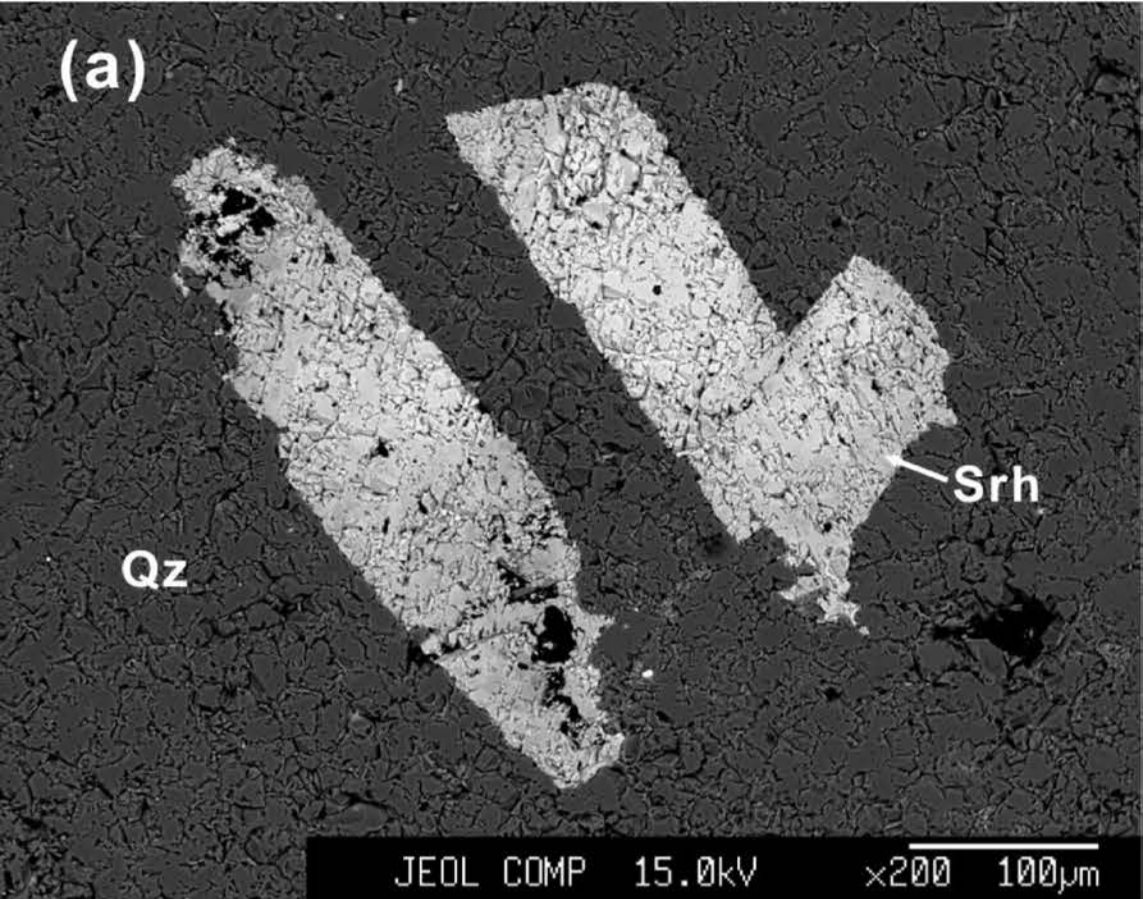
319 **FIGURE 3.** The crystal structure of strontiohurlbutite. Note: PO₄ tetrahedra in dark gray; BeO₄
320 tetrahedra in gray; circle for Sr atoms.

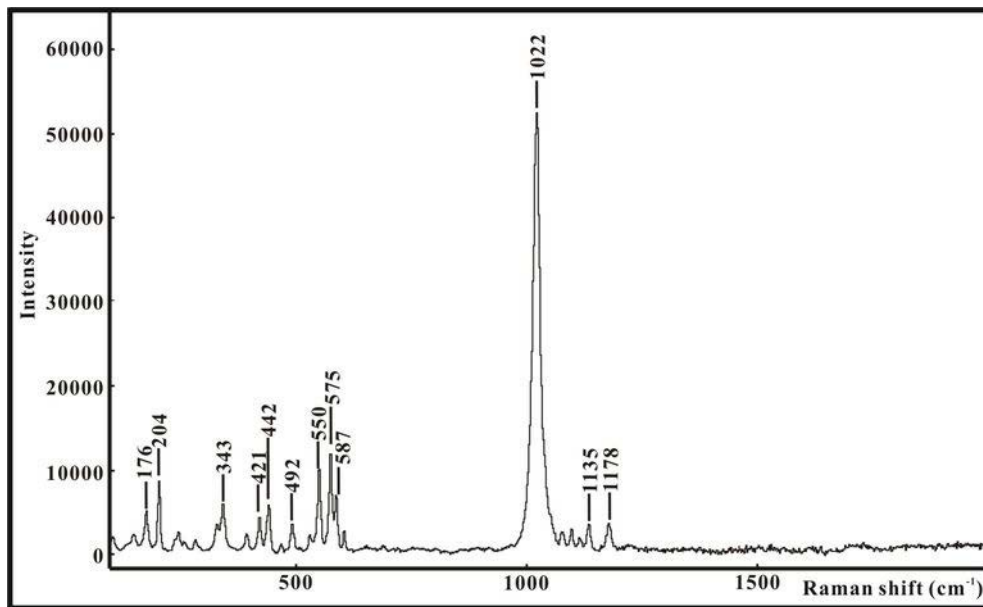
321

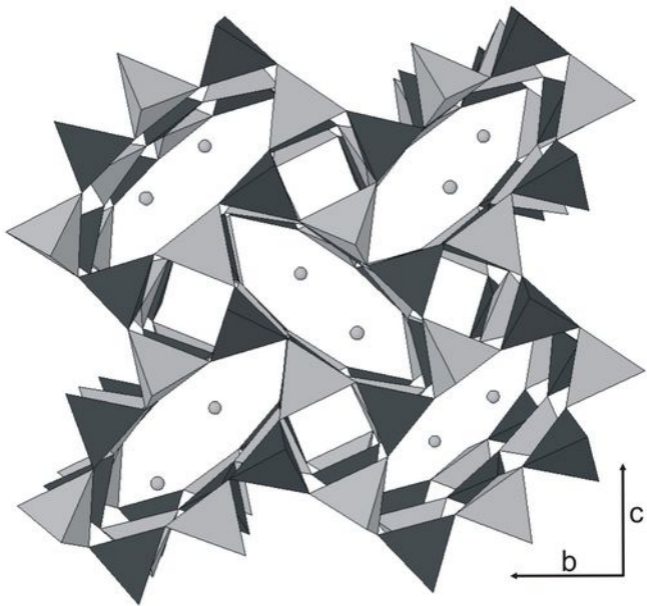
322 **FIGURE 4.** Chains and rings in the crystal structure of strontiohurlbutite (PO₄ tetrahedra: dark
323 gray; BeO₄ tetrahedra: gray). (a) 4-membered ring with the pattern UUDD; (b) 8-membered
324 ring with the pattern DDUDUUDU; (c) double-crankshaft chain aligned along the *a* axis.

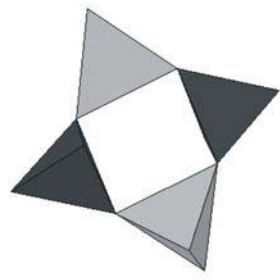
325

337

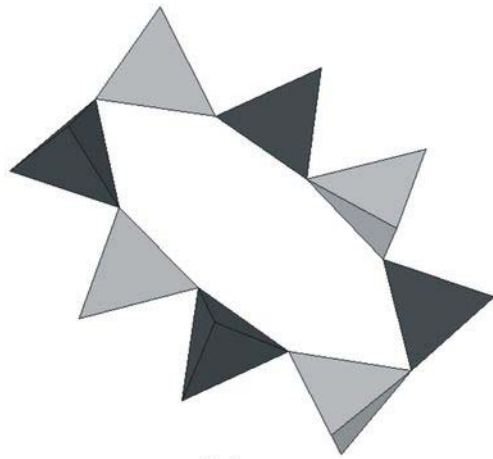




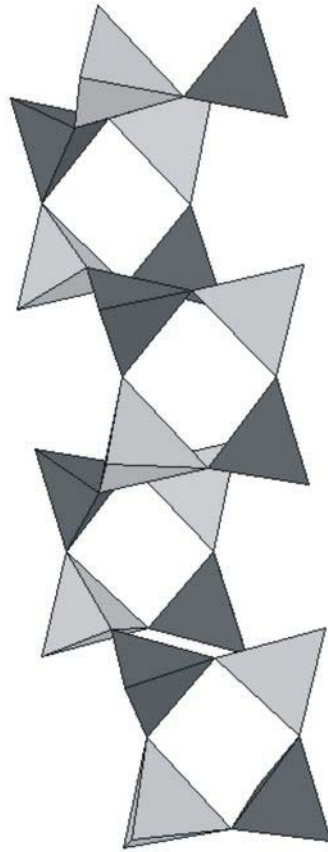




(a)



(b)



(c)

TABLE 1. Representative electron-microprobe results of strontiohurlbutite from the Nanping No. 31 pegmatite dyke

	Strontiohurlbutite from Nanping No. 31 pegmatite						Average	Ideal strontiohurlbutite
	NP-66 (zone I)		NP-14 (zone II)		NP-54 (zone IV)			
P ₂ O ₅ wt. %	50.54	50.54	50.54	52.73	50.75	51.20	51.05	48.02
SrO	29.04	29.67	30.02	28.88	30.61	27.57	29.30	35.06
BeO*	17.71	17.71	17.71	17.71	17.71	17.71	17.71	16.92
CaO	0.07	0.17	0.15	0.18	1.80	3.10	0.91	
BaO	1.21	0.87	1.18	0.18	0.18	0.22	0.64	
Total	98.11	98.55	99.23	99.81	100.98	99.81	99.61	100.00
Structural formulas calculated on the basis of O=8 atoms								
P <i>apfu</i>	2.051	2.047	2.043	2.087	2.025	2.036	2.048	2.000
Sr	0.807	0.823	0.831	0.783	0.837	0.751	0.805	1.000
Be	2.039	2.035	2.031	1.989	2.006	1.999	2.016	2.000
Ca	0.004	0.009	0.008	0.009	0.091	0.156	0.046	-
Ba	0.023	0.016	0.022	0.003	0.003	0.004	0.012	-

*: BeO was measured by SIMS.

TABLE 2. Powder X-ray diffraction data for strontiohurlbutite

<i>h</i>	<i>k</i>	<i>l</i>	<i>d</i> _{meas} (Å)	<i>d</i> _{calc} (Å)	<i>I</i> _{rel}
0	1	1	6.150	6.150	9
1	1	0	5.985	5.981	3
2	1	0	3.653	3.657	5
1	2	1	3.554	3.555	100
2	1	1	3.355	3.354	51
0	2	2	3.073	3.075	38
1	3	0	2.810	2.809	27
0	1	3	2.678	2.681	9
1	1	3	2.542	2.542	67
0	2	3	2.380	2.383	26
3	2	0	2.294	2.295	1
2	1	3	2.230	2.227	42
3	2	$\bar{1}$	2.215	2.215	87
2	3	$\bar{2}$	2.083	2.086	26
2	2	3	2.046	2.047	54
3	3	0	1.994	1.994	19
1	1	4	1.986	1.986	13
3	2	3	1.776	1.777	16
2	2	4	1.721	1.722	21
1	4	3	1.714	1.715	32
0	1	5	1.655	1.656	11
3	$\bar{1}$	$\bar{4}$	1.627	1.627	31
3	1	4	1.623	1.625	6
1	$\bar{2}$	$\bar{5}$	1.549	1.549	10
4	2	3	1.531	1.532	4
5	1	$\bar{3}$	1.376	1.375	6

TABLE 3. Crystal data and refinement parameters for strontiohurlbutite

Crystal size (mm)	0.35 × 0.35 × 0.18
Color	Light blue
Space group	<i>P2₁/c</i>
<i>a</i> , <i>b</i> , <i>c</i> (Å)	7.997(1), 8.979(1), 8.420(1)
β (°)	90.18(1)
<i>V</i> (Å ³)	604.7(1)
<i>Z</i>	4
<i>D</i> (calc) (g/cm ³)	3.101
2 θ _{min} , 2 θ _{max}	6.64°, 58.18°
Range of indices	−10 ≤ <i>h</i> ≤ 10, −12 ≤ <i>k</i> ≤ 12, −11 ≤ <i>l</i> ≤ 11
Measured intensities	26214
Unique reflections	1566
Independent non-zero [<i>I</i> > 2 σ (<i>I</i>)] reflections	1473
μ (mm ^{−1})	9.451
Refined parameters	118
<i>R</i> ₁ [<i>F</i> _o > 2 σ (<i>F</i> _o)]	0.0197
<i>R</i> ₁ (all)	0.0234
<i>wR</i> ₂ (all)	0.0467
<i>S</i> (goodness of fit)	1.106
Max Δ / σ in the last l.s. cycle	0.001
Max peak and hole in the final ΔF map (e/Å ³)	+0.44 and −0.42

TABLE 4. Atomic coordinates and displacement parameters (\AA^2) for strontiohurlbutite

Atom	<i>x</i>	<i>y</i>	<i>z</i>	<i>U</i> ₁₁	<i>U</i> ₂₂	<i>U</i> ₃₃	<i>U</i> ₂₃	<i>U</i> ₁₃	<i>U</i> ₁₂	<i>U</i> _{eq}
Sr	0.25553(2)	0.91255(2)	0.10887(2)	0.0093(1)	0.0075(1)	0.0092(1)	-0.00060(7)	-0.00046(7)	0.00024(7)	0.00867(7)
P1	0.56332(7)	0.69579(6)	-0.06627(6)	0.0073(2)	0.0049(2)	0.0049(2)	0.0001(2)	-0.0002(2)	0.0001(2)	0.0057(1)
P2	0.06219(7)	0.58553(6)	0.23174(6)	0.0070(2)	0.0060(2)	0.0046(2)	-0.0003(2)	-0.0004(2)	-0.0002(2)	0.0059(1)
Be1	0.4288(3)	0.9193(3)	-0.2734(3)	0.009(1)	0.008(1)	0.008(1)	0.000(1)	-0.000(1)	0.001(1)	0.0080(5)
Be2	-0.0739(3)	0.6931(3)	-0.0633(3)	0.009(1)	0.009(1)	0.007(1)	0.001(1)	-0.001(1)	-0.000(1)	0.0084(5)
O1	0.4369(2)	0.6818(2)	0.0703(2)	0.0101(7)	0.0093(7)	0.0075(7)	0.0009(6)	0.0014(6)	0.0008(6)	0.0090(3)
O2	0.2404(2)	0.9069(2)	-0.1991(2)	0.0074(7)	0.0162(8)	0.0071(7)	0.0005(6)	0.0000(6)	-0.0004(6)	0.0102(3)
O3	0.5490(2)	0.8580(2)	-0.1277(2)	0.0106(7)	0.0062(7)	0.0082(7)	0.0018(6)	-0.0025(6)	0.0001(6)	0.0083(3)
O4	0.7383(2)	0.6626(2)	-0.0085(2)	0.0082(7)	0.0111(8)	0.0119(7)	0.0029(6)	-0.0001(6)	-0.0003(6)	0.0104(3)
O5	0.4906(2)	1.0885(2)	-0.3003(2)	0.0143(7)	0.0067(7)	0.0074(7)	0.0018(5)	-0.0028(6)	-0.0011(6)	0.0095(3)
O6	-0.0063(2)	0.9273(2)	0.3062(2)	0.0141(8)	0.0062(7)	0.0084(7)	0.0009(5)	0.0023(6)	0.0007(6)	0.0096(3)
O7	0.0564(2)	0.6876(2)	0.0871(2)	0.0102(7)	0.0087(7)	0.0068(7)	0.0015(6)	-0.0020(6)	-0.0014(6)	0.0085(3)
O8	-0.0555(2)	0.8622(2)	-0.1352(2)	0.0090(7)	0.0067(7)	0.0084(7)	0.0017(6)	0.0022(6)	0.0004(6)	0.0080(3)

TABLE 5. Selected bond distances (Å) and angles (°) for strontiohurlbutite

P1-O3	1.549(2)	O2-Be1-O3	103.2(2)
P1-O5	1.541(2)	O5-Be1-O2	113.6(2)
P1-O4	1.509(2)	O5-Be1-O3	103.9(2)
P1-O1	1.538(2)	O1-Be1-O2	108.4(2)
Mean	1.535	O1-Be1-O3	113.4(2)
		O1-Be1-O5	113.9(2)
O5-P1-O3	108.92(8)	Mean	109.39
O4-P1-O3	111.16(9)		
O4-P1-O5	111.62(9)	Be2-O8	1.642(3)
O4-P1-O1	110.68(8)	Be2-O7	1.638(3)
O1-P1-O3	106.14(8)	Be2-O4	1.597(3)
O1-P1-O5	108.12(9)	Be2-O6	1.635(3)
Mean	109.44	Mean	1.628
P2-O8	1.539(2)	O7-Be2-O8	104.8(2)
P2-O2	1.540(2)	O7-Be2-O8	110.6(2)
P2-O7	1.525(2)	O7-Be2-O8	111.6(2)
P2-O6	1.523(2)	O7-Be2-O8	113.2(2)
Mean	1.531	O7-Be2-O8	109.5(2)
		O7-Be2-O8	106.8(2)
O8-P2-O2	106.21(8)	Mean	109.40
O7-P2-O8	112.43(9)		
O7-P2-O2	107.53(9)	Sr-O8	2.588(2)
O6-P2-O8	104.89(9)	Sr-O8'	3.253(2)
O6-P2-O2	113.03(9)	Sr-O2	3.295(2)
O6-P2-O7	112.64(9)	Sr-O2'	2.596(2)
Mean	109.45	Sr-O3	2.591(2)
		Sr-O3'	3.122(2)
Be1-O2	1.637(3)	Sr-O5	2.588(2)
Be1-O3	1.651(3)	Sr-O7	2.579(2)
Be1-O5	1.614(3)	Sr-O6	2.680(2)
Be1-O1	1.600(3)	Sr-O1	2.551(2)
Mean	1.627	Mean	2.784

Table 6. Bond valence sums for strontiohurlbutite

	Sr	P1	P2	Be1	Be2	Σ
O1	0.31	1.23		0.55		2.10
O2	0.27 0.04		1.23	0.50		2.05
O3	0.28 0.07	1.20		0.48		2.03
O4		1.33			0.56	1.89
O5	0.28	1.23		0.53		2.04
O6	0.22		1.29		0.50	2.01
O7	0.29		1.28		0.50	2.07
O8	0.28 0.05		1.23		0.49	2.06
Σ	2.09	5.00	5.04	2.07	2.05	

TABLE 7. Comparison of the physical properties of strontiohurlbutite and hurlbutite

	Strontiohurlbutite	Hurlbutite (Mrose 1952)
Color	light blue	colorless to greenish
Structural formula	$\text{SrBe}_2(\text{PO}_4)_2$	$\text{CaBe}_2(\text{PO}_4)_2$
Space group	$P2_1/c$	$P2_1/a$
<i>a</i>	7.997 (1) Å	8.29 Å
<i>b</i>	8.979 (1) Å	8.80 Å
<i>c</i>	8.420 (1) Å	7.81 Å
β	90.18 (1)°	90.5°
<i>V</i>	604.7 (1) Å ³	570 Å ³
<i>Z</i>	4	4
Density	3.101* g/cm ³ (calc)	2.90* g/cm ³ (calc)

* Density calculation based on the empirical formula